Global and Planetary Change 127 (2015) 79–90

Contents lists available at ScienceDirect

Global and Planetary Change

journal homepage: www.elsevier.com/locate/gloplacha

Carbon isotope records reveal synchronicity between carbon cycle perturbation and the "Carnian Pluvial Event" in the Tethys realm (Late Triassic)

Jacopo Dal Corso [a,*], Piero Gianolla [b], Robert J. Newton [c], Marco Franceschi [a], Guido Roghi [d], Marcello Caggiati [b], Béla Raucsik [e], Tamás Budai [f], János Haas [g], Nereo Preto [a]

[a] Dipartimento di Geoscienze, Università degli Studi di Padova, Via Gradenigo 6, 35131 Padova, Italy
[b] Dipartimento di Fisica e Scienze della Terra, Università degli Studi di Ferrara, via Saragat 1, 44100 Ferrara, Italy
[c] School of Earth and Environments, University of Leeds LS2 9JT, Leeds, UK
[d] Istituto di Geoscienze e Georisorse (IGG-CNR), via Gradenigo 6, 35131 Padova, Italy
[e] Department of Mineralogy, Geochemsitry and Petrology, University of Szeged, Egyetem utca 2H-6722, Szeged, Hungary
[f] Geological and Geophysical Institute of Hungary, Stefánia út 14. H-1143, Budapest, Hungary
[g] MTA-ELTE Geological, Geophysical and Space Science Research Group, Hungarian Academy of Sciences Pázmány P. sétány 1/c H-1117, Budapest, Hungary

ARTICLE INFO

Article history:
Received 15 September 2014
Received in revised form 13 January 2015
Accepted 22 January 2015
Available online 29 January 2015

Keywords:
Carnian Pluvial Event
Late Triassic
Carbon isotope
Oxygen depletion
Carbonate crisis

ABSTRACT

In the early Late Triassic a period of increased rainfall, named the Carnian Pluvial Event (CPE), is evidenced by major lithological changes in continental and marine successions worldwide. The environmental change seems to be closely associated with a negative carbon isotope excursion that was identified in a stratigraphic succession of the Dolomites (Italy) but the temporal relationship between these phenomena is still not well defined. Here we present organic-carbon isotope data from Carnian deep-water stratigraphic sections in Austria and Hungary, and carbonate petrography of samples from a marginal marine section in Italy. A negative 2–4‰ $\delta^{13}C$ shift is recorded by bulk organic matter in the studied sections and is coincident with a similar feature highlighted in higher plant and marine algal biomarker carbon-isotope records from the Dolomites (Italy), thus testifying to a global change in the isotopic composition of the reservoirs of the exchangeable carbon. Our new observations verify that sedimentological changes related to the CPE coincide with the carbon cycle perturbation and therefore occurred synchronously within the western Tethys. Consistent with modern observations, our results show that the injection of ^{13}C-depleted CO_2 into the Carnian atmosphere–ocean system may have been directly responsible for the increase in rainfall by intensifying the Pangaean mega-monsoon activity. The consequent increased continental weathering and erosion led to the transfer of large amounts of siliciclastics into the basins that were rapidly filled up, while the increased nutrient flux triggered the local development of anoxia. The new carbonate petrography data show that these changes also coincided with the demise of platform microbial carbonate factories and their replacement with metazoan driven carbonate deposition. This had the effect of considerably decreasing carbonate deposition in shallow water environments.

1. Introduction

The peculiar Late Triassic paleogeographic setting, with a single supercontinent (Pangaea) surrounded by a single vast ocean (Panthalassa), and enclosing a much smaller ocean (Tethys), created the conditions for a global-scale "mega-monsoon". This climate was characterized by a marked seasonality, upwelling along tropical coasts and arid to semi-arid climates over the continental interior (Kutzbach and Gallimore, 1989; Sellwood and Valdes, 2006; Preto et al., 2010; Stefani et al., 2010). This monsoonal climate was perturbed during a geologically short-lived period of extreme rainfall, the so-called Carnian Pluvial Event (CPE), that caused large-scale changes in many depositional environments, from continental to deep-water settings (Fig. 1) (Schlager and Schöllnberger, 1974; Simms and Ruffell, 1989; Simms et al., 1995; Furin et al., 2006; Arche and López-Gómez, 2014 and references therein).

Paleosols indicative of tropical humid climate developed in formerly semi-arid environments of continental Pangaea and particulate transport by rivers increased (e.g. Breda et al., 2009; Arche and López-Gómez, 2014; Franz et al., 2014). Palynological analyses show an increase of hygrophytic forms (Azonotriletes spores) that reflect a floral change towards plant communities adapted to a more humid environment, e.g. ferns, equisetaleans and cycadaleans (Roghi, 2004; Roghi et al., 2010). Shallow-water carbonate production was put into crisis, oxygen-depleted conditions were established, hundreds of meters of coarse siliciclastic, mixed terrigenous-carbonate sediments and black

* Corresponding author.
E-mail addresses: jacopo.dalcorso@unidp.it, jacopo.dalcorso@gmail.com (J. Dal Corso).

http://dx.doi.org/10.1016/j.gloplacha.2015.01.013
0921-8181/

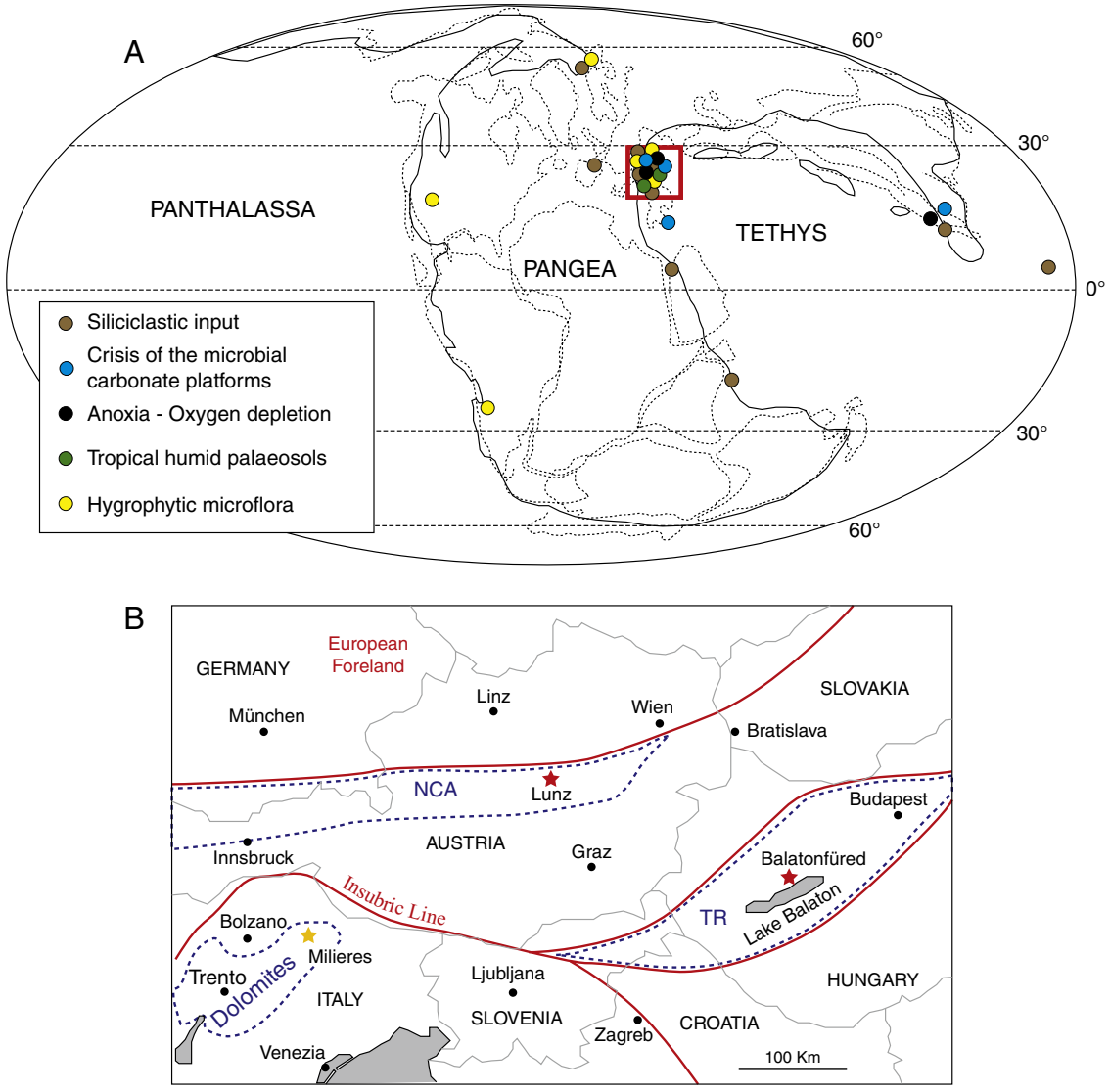

Fig. 1. A) Late Triassic palaeogeography and location of the areas where the sedimentological and paleobotanical evidences of the Carnian Pluvial Event are reported. Red square: paleogeographic position of the study area. Figure modified after Nakada et al. (2014) and the following selected studies. Reviews and inter-regional studies: Preto et al. (2010); Roghi et al. (2010); Arche and López-Gómez (2014). Southern Alps: Preto and Hinnov (2003); Keim et al. (2006); Breda et al. (2009). Northern Calcareous Alps (Austria): Hornung et al. (2007a, 2007b). Transdanubian Range (Hungary): Rostási et al. (2011); Haas et al. (2012). Lagonegro basin (Southern Italy): Rigo et al. (2007). Anatolian terrane (Turkey): Lukeneder et al. (2012). Levant margin (Israel): Bialik et al. (2013). Tamba–Mino–Ashio Belt (Japan): Nakada et al. (2014). South China Block (China): Wang et al. (2008). B) Map of the study area and major tectonic controls. Red stars = studied sections. Yellow star = section studied in Dal Corso et al. (2012).

shales were rapidly deposited into marginal marine basins (e.g. Keim et al., 2006; Breda et al., 2009; Rostási et al., 2011). Carbonate sedimentation significantly reduced or halted completely in pelagic settings, where a rise of the carbonate compensation depth (CCD) has been hypothesized (Hornung et al., 2007a; Neri et al., 2007; Rigo et al., 2007; Preto et al., 2010; Rostási et al., 2011; Haas et al., 2012; Lukeneder et al., 2012; Nakada et al., 2014).

A negative carbon isotope excursion (CIE) recorded by terrestrial and marine biomarkers (4‰) and bulk organic matter (2‰) has been found in a Julian (lower Carnian) marine sequence of the Dolomites (Southern Alps, Italy), roughly at the onset of the CPE. The excursion testifies to an injection of ^{13}C-depleted CO_2 into the atmosphere–ocean system that is thought to be linked to the outpouring of the Wrangellia Large Igneous Province flood basalts (Dal Corso et al., 2012; Xu et al., 2014). So far, the negative organic-CIE has not been replicated outside the Dolomites, and the temporal relationships between the carbon cycle perturbation and the effects of the CPE on depositional systems indicated by the sedimentological changes are not yet well constrained.

In this paper, high-resolution carbon isotope records of bulk organic matter from two stratigraphic sections in the Lunz area (Northern Calcareous Alps, Austria), from a borehole in Hungary (Balatonfüred Bfü-1) and from the carbonates of the Milieres section (Dolomite, Italy) are presented. Point counting was carried out in thin sections from the Dolomites section to highlight changes in the source of carbonate to the basin. The carbon isotope curves are correlated with the existing biomarker and bulk organic matter records from the Dolomites (Southern Alps, Italy) and coupled to sedimentological data in order to shed light onto the temporal relationships between the input of ^{12}C into the atmosphere-ocean system, the increased flux of siliciclastic sediment, the establishment of oxygen-depleted conditions in marginal basins, and the crisis of shallow-water microbial carbonate factories.

2. Geological setting

During the Carnian, all the studied basins were located in the western Tethys (Fig. 1A; Csontos and Vörös, 2004). The early Carnian stratigraphy

of the Lunz nappe of the Northern Calcareous Alps (Austria, Fig. 1B for location) is a succession of carbonate–siliciclastic sedimentary rocks that records the evolution of the basin from deep-water to delta and carbonate shelf (Rüffer and Bechstädt, 1998; Fig. 2). The Upper Ladinian–Lower Julian deep-water nodular limestones of the Reifling Fm. are overlain by the laminated dark mudstones and grainstones of the Göstling Fm., which testify to decreasing carbonate input and increasing oxygen depletion in the basin (Hornung et al., 2007b). The lithological change between the Reifling and the Göstling Fms. occurs approximately at the Julian 1–Julian 2 boundary, corresponding to the *Trachyceras–Austrotrachyceras* ammonoid zones boundary (*sensu* Krystyn, 1991 and Hornung et al., 2007b; Supplementary Data). Above this level, an increase in clayey interbeds precedes the transition to the Reingraben Fm., a succession of shales that contains sporomorphs of the Julian 2 (*Aulisporites astigmosus* assemblage; Roghi et al., 2010) (Fig. 2 and Supplementary Data). The proportion of shale and dark mudstone increases towards the overlying coarse terrigenous Lunz Fm. (Köppen, 1997), consisting of deltaic sandstones and siltstones with abundant plant debris (Pott et al., 2008). The infilling of the basins of the Northern Calcareous Alps was completed by deposition of the siliciclastic succession (ca. 400 m-thick) of the Lunz Fm., which was followed by carbonate shelf sedimentation of the Opponitz Fm. (Fig. 2).

In the Balatonfüred borehole Bfü-1 (Hungary, Fig. 1B), the Carnian sedimentary succession records the infilling of the basins and a general evolution from pelagic to shallow-water paleoenvironments. The early Carnian Füred Fm. consists of a succession of pelagic cherty nodular limestones poor in macrofossils: Ammonoids (*Trachyceras* zone; Julian 1), bivalves, and brachiopods occur scarcely and early Carnian conodonts are occasionally found (supplementary data). The uppermost part of the Füred Fm. — lowermost part of the Veszprém Fm. consists of clay-rich limestone and yields the ammonoids *Sirenites* sp. and *Neoprotrachyceras* spp. (Budai et al., 1999) that belong to the *Austrotrachyceras* ammonoid zone (Julian 2; Krystyn, 1978; Lukeneder and Lukeneder, 2013). An increase in the fine siliciclastic fraction

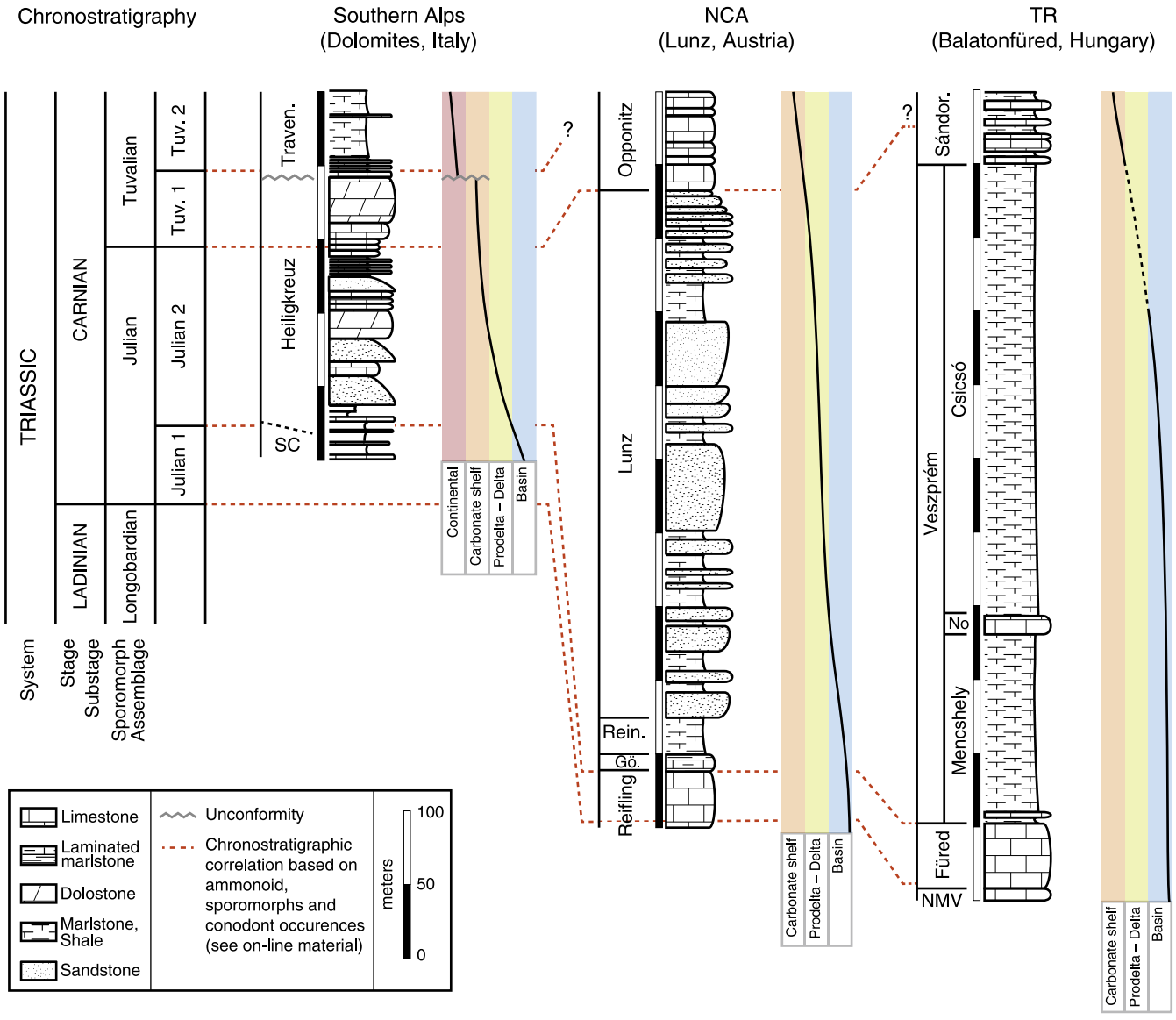

Fig. 2. Schematic stratigraphy of the Carnian successions of Transdanubian Range (Hungary) and the Northern Calcareous Alps (Austria) showing the correlation of the studied sections with the Dolomites in Italy. Correlation is based on biostratigraphic data from Krystyn (1991), Budai et al. (1999), Hornung et al. (2007a), Roghi et al. (2010) and references therein. See Supporting Data for full discussion of the biostratigraphic constrains and supplementary figures. In the Northen Calcareous Alps (NCA) and the Transdanubian Range (TR) the prevailing carbonate sedimentation was suddenly interrupted during the Julian, ca. at the Julian 1–Julian 2 boundary and replaced with a siliciclastic sedimentation that in a relatively short time (within the Julian 2) filled up the basins of the Carnian western Tethys. SC = San Cassian Fm., Traven. = Travenanzes Fm., Gö = Göstling Fm., Rein. = Reingraben Fm., NMV = Nemesvamos Fm., No = Nosztor Limestone Mb., Sándor = Sándorhegy Fm.

marks the transition to the Mencshely Member of the Veszprém Fm. (Fig. 2), and is characterized by dark-gray thin-bedded laminated and bioturbated marls with silt–sand intercalations and increasing kaolinite content, documenting more humid conditions related to the onset of the CPE (Rostási et al., 2011). The following 10–12 m thick Nosztor Limestone Member of the Veszprém Fm. contains ammonoids of the *Austrotrachyceras* ammonoid zone (Budai et al., 1999). It is overlain by gray to dark gray marls and clays of the Csicsó Member, lithologically very similar to, and almost indistinguishable from the Mencshely Member (Budai et al., 1999). The basins of the Transdanubian Range were gradually filled until the onset of the shallow-water carbonate shelf deposition of the Sándorhegy Fm. (Fig. 2). The Veszprém Fm. bears sporomorphs of the *Aulisporites astigmosus* assemblage (Góczán et al., 1991).

In the Dolomites (Milieres, Southern Alps, Italy; Fig. 1B), the complex Carnian topography, consisting of high-relief carbonate platforms ("Cassian" platforms) surrounded by deep basins (San Cassiano Fm.), was flattened by the deposition of the Heiligkreuz Fm. during the CPE (Neri et al., 2007; Stefani et al., 2010; Fig. 2). The Heiligkreuz Fm. is a ca. 150 m thick sedimentary succession of prodelta–delta to coastal–paralic marls, limestones, and sandstones, which is overlain by the Travenanzes Fm. (Fig. 2), representing tidal-flat, sabkha and alluvial-plain depositional environments of the late Carnian southwestern Tethys (Breda and Preto, 2011). The age of the succession is well constrained by ammonoid and sporomorph biostratigraphy (Supplementary Data).

A more detailed discussion and additional figures about the biostratigraphic constrains of the studied sections are given as Supporting Data.

3. Methods

3.1. Studied stratigraphic sections

Two stratigraphic sections in the Lunz area (Northern Calcareous Alps) were selected for carbon isotope analysis of total organic carbon ($\delta^{13}C_{TOC}$) and sampled across the sedimentological changes that mark the onset of the CPE: Göstling section (47°48′22.6″N, 14°57′3.44″E) and Polzberg section (47°53′4.09″N; 15°4′28.17″E) (Fig. 1B). In the Göstling section the Reifling Fm. and part of the Göstling Fm. are exposed, while the Polzberg section encompasses the uppermost part of the Göstling Fm. and the lower part of the Reingraben Fm. (the composite section is shown in Fig. 3A). In Hungarian the uppermost Ladinian–Carnian portion of core Bfü-1 was sampled for bulk organic matter carbon isotope analysis. The Bfü-1 borehole was collected near the village of Balatonfüred (Fig. 1) in 1977 and is now stored at Szépvízér (repository of the Hungarian Office for Mining and Geology). The studied portion of the Bfü-1 borehole (Fig. 3B) encompasses the entire Füred Fm. and the lowermost part of the Veszprém Marl Fm. (Mencshely Marl Member) that corresponds to the onset of the CPE (Rostási et al., 2011). In the Dolomites, the basal part of the Milieres section has been sampled for carbonate carbon and oxygen isotope ($\delta^{13}C_{CARB}$ and $\delta^{18}O_{CARB}$) analysis, and to study the petrography of the calcarenites found across the negative organic-CIE previously identified by Dal Corso et al. (2012) (Fig. 4). The Milieres section encompasses the uppermost San Cassiano Fm. — lowermost Heiligkreutz Fm. (Dal Corso et al., 2012). All the collected samples are stored at the Department of Geosciences of the University of Padova (Italy).

3.2. $\delta^{13}C_{TOC}$ analysis

Sixty-nine samples from the Lunz sections (47 from Göstling and 22 from Polzberg) and 53 samples from Bfü-1 borehole have been analyzed for $\delta^{13}C_{TOC}$ (Fig. 3).

Rock samples were cleaned with deionized water to remove superficial impurities, then oven-dried at 40° and crushed in an agate mortar. To remove carbonates, the powder was placed in a polypropylene Falcon tube and acid-washed with 10% HCl. Residual powder was then rinsed with deionized water. $\delta^{13}C_{TOC}$ analyses were carried out at the School of Earth and Environment, University of Leeds, UK. $\delta^{13}C_{TOC}$ analyses of the samples from the Transdanubian Range (Hungary) have been replicated at the Department of Geosciences, University of Padova, Italy.

At Leeds, the $\delta^{13}C_{TOC}$ analyses were performed using an Isoprime mass spectrometer coupled to an Elementar Pyrocube elemental analyzer. Samples were weighed into tin cups in sufficient quantity to produce peaks of between 1 and 10 nA. The encapsulated samples were converted to CO_2 by combustion at 1150 °C in the presence of pure oxygen (N5.0) injected into a stream of helium (CP grade). Quantitative conversion to CO_2 was achieved by passing the gases through tungstic oxide also at 1150 °C. Excess oxygen was removed by reaction with hot copper wires at 850 °C, and water was removed in a Sicapent trap. All solid reagents were sourced from Elemental Microanalysis, UK, and all gases were sourced from BOC, UK. N_2 continued through the system unchecked, while CO_2 and SO_2 were separated using temperature controlled adsorption/desorption columns. The $\delta^{13}C$ of the sample is derived from the integrated mass 44, 45 and 46 signals from the pulse of sample CO_2, compared to those in an independently introduced pulse of CO_2 reference gas (CP grade). These ratios were calibrated to the international VPDB scale using in-house C4 sucrose and urea standards. These were assigned values of -11.93 ± 0.24‰ and -46.83 ± 0.22‰ respectively as the result of a calibration using six replicates of each of the following international standards (assigned values in brackets): IAEA-LSVEC (−46.479‰), IAEA-CH7 (−31.83‰), IAEA-CH6 (−10.45‰) and IAEA-CO1 (+2.48‰). The precision obtained for repeat analysis was better than ± 0.2‰ (σ).

At the Department of Geosciences, University of Padova, $\delta^{13}C_{TOC}$ analyses were performed on a Thermo Scientific Delta V Advantage Isotope Ratio Mass Spectrometer in continuous flow mode, coupled with a Flash 2000 Elemental Analyzer and a ConFlo IV interface. Between 1 and 5 mg of sample was wrapped in a tin capsule and fed to the Elemental Analyzer; the resulting CO_2 gas was analyzed by the Mass Spectrometer. A blank correction was introduced on the base of a long-term mean of >30 tin cap analyses, and the results were calibrated against repeated analyses of two international standards (IAEA-CH6, −10.449‰, and IAEA-CH7, −32.151‰). The long-term reproducibility, estimated on blank-corrected and calibrated analyses of an internal standard (C3 plants sucrose), is better than 0.2‰ (1σ).

3.3. $\delta^{13}C_{CARB}$ and $\delta^{18}O_{CARB}$ analysis

For carbonate carbon and oxygen isotope analyses, the Thermo Scientific Delta V Advantage Isotope Ratio Mass Spectrometer of the Department of Geosciences, University of Padova was used. Carbonate powder was obtained from bulk samples with a dental drill and ca. 0.2–0.3 mg was weighted in exetainer vials. CO_2 was developed at 70 °C by complete reaction with pure H_3PO_4 in a Gasbench II device connected to the spectrometer. Repeated analyses of an internal standard (sieved Carrara marble, calibrated against the primary reference carbonate NBS 19, $\delta^{13}C = 1.95$‰ $\delta^{18}O = -2.20$‰) were run along the samples. The long term reproducibility of this setup, measured on the internal standard, is better than 0.1‰ (1σ) for both carbon and oxygen.

3.4. Carbonate petrography

Point counting of allochtonous carbonates was performed on thin sections from Milieres (Dolomites), which is the most proximal among the studied sections, to monitor changes in the source of carbonate to the basin. Fourteen thin sections (30 μm thick) were examined under a polarized microscope at the ZMT (Leibniz Center for Tropical Marine Ecology) of Bremen, Germany. An average of 540 points per thin section were evaluated in order to obtain statistically significant of modal abundances (Van der Plas and Tobi, 1965). The grid step was

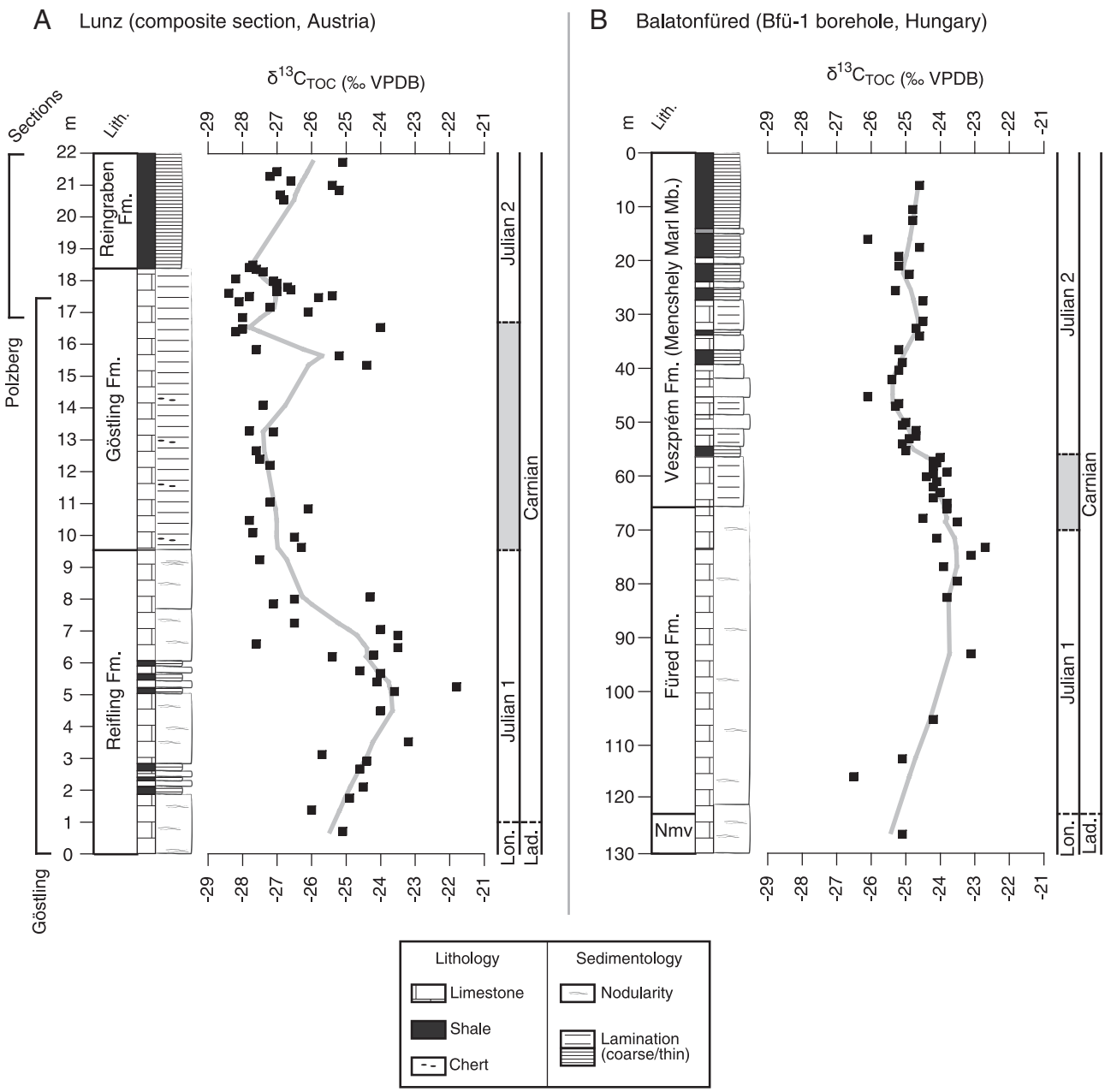

Fig. 3. Detailed stratigraphic logs and organic-carbon isotope data from Lunz (Northern Calcareous Alps) and Balatonfüred (Bfü-1 core, Transdanbian Range). A ca. 3‰ early Carnian positive $\delta^{13}C_{TOC}$ trend is suddenly interrupted by a 2‰–4‰ negative CIE which onset is coincident with the major sedimentological changes linked to the abrupt rise of rainfall and continental weathering of the Carnian Pluvial Event. A weighted least squares function (±15%) was applied to fit a curve to the data. Nmv = Nemesvamos Fm (Ladinian).

chosen in order to be larger than the large majority of grains. Two samples showed uneven grain size distribution within the thin section; in these cases, separate point counting was performed for the different parts. Four additional thin sections of microbial boundstone were not point-counted, but their position is annotated in Fig. 4.

4. Results

4.1. $\delta^{13}C_{TOC}$ data

$\delta^{13}C_{TOC}$ values at Lunz range from −28.4‰ to −21.8‰, while those from the Bfü-1 borehole range from −26.5‰ to −22.7‰. Both sections exhibit a lower Carnian 2‰–3‰ increase in the $\delta^{13}C_{TOC}$ (Fig. 3). The positive trend is suddenly interrupted (at 70–80 m in the Bfü-1 borehole and at 5–6 m at Lunz) as the $\delta^{13}C_{TOC}$ shifts towards more negative values (2–4‰ negative CIE, Figs. 3 and 5). In both sections the negative CIE occurs over the Julian 1–Julian 2 boundary (Fig. 5; supplementary data). The negative CIE begins in the uppermost part of the Füred Fm. at Bfü-1 and the upper Reifling Fm. at Lunz. Carbon isotope values remain depressed throughout most of the thin-bedded clay-rich limestone and shales of the basal Veszprém Fm. (Bfü-1) and the Göstling and Reingraben Fms. (Lunz) (Fig. 3). All carbon isotope data are available as Supplementary Data (Tables 1S and 2S).

4.2. $\delta^{13}C_{CARB}$ and $\delta^{18}O_{CARB}$ data

Carbonate carbon isotope data vary between 1.7‰ and 3.6‰ with a mean of 2.9 ± 0.4‰ (Fig. 4). Carbonate oxygen isotope data vary between −4.9‰ and −2.3‰ with a mean of −3.8 ± 0.9‰ (Fig. 4). $\delta^{13}C_{CARB}$ and $\delta^{18}O_{CARB}$ show little correlation (R^2 = 0.2; Fig. 4 and Supplementary Data for $\delta^{13}C_{CARB}$ *vs.* $\delta^{18}O_{CARB}$ cross-plot), which points to little diagenetic effect on the original carbonate isotopic signature

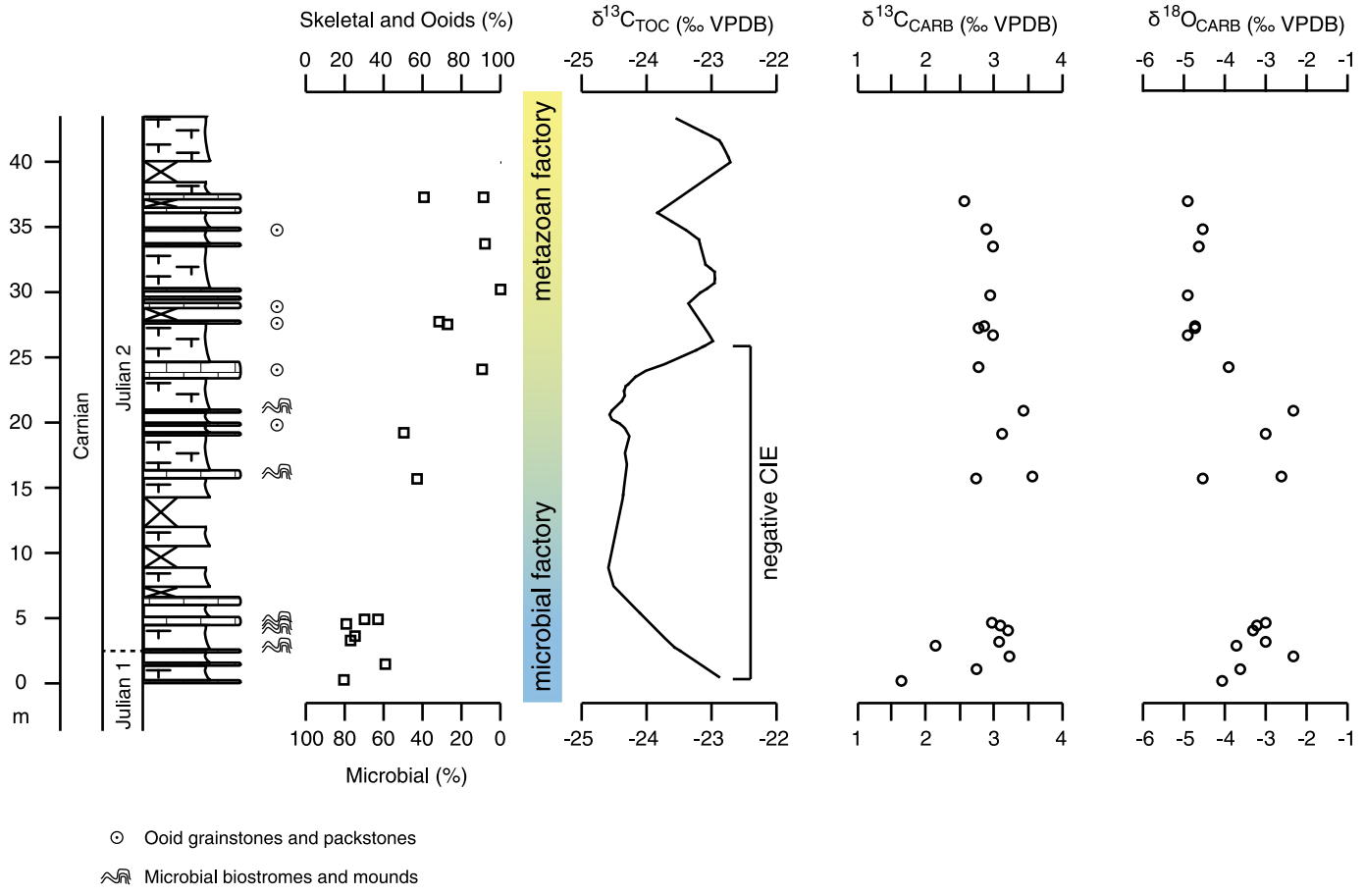

Fig. 4. Modal abundance of carbonate grains of packstone and grainstone beds, organic-carbon isotope negative excursion (Dal Corso et al., 2012) and carbonate-carbon and oxygen isotope data from Mileres section in the Dolomites, Italy (Fig. 1). The composition of grainstones and packstones changes dramatically along the Milieres section, from facies that are dominated by microbial carbonates at its base, to oolites and skeletal grainstones with less than 10% of microbial-derived grains at its top. This sharp transition coincides with the negative CIE at Milieres. Carbonate carbon isotope data do not parallel those of bulk organic matter pointing to diagenetic and/or facies control on the carbonate $\delta^{13}C$ signature.

(Marshall, 1992). $\delta^{13}C_{CARB}$ data show no significant trends and do not parallel organic carbon isotope data from the same section (Fig. 4). All $\delta^{13}C_{CARB}$ and $\delta^{18}O_{CARB}$ data from Milieres section in the Dolomites are available as Supplementary Data (Table 3S).

4.3. Carbonates

The relative modal abundances of various carbonate components of the packstone and grainstone beds of the section at Milieres in the Dolomites (Fig. 1) reflect those of the main carbonate producers in adjacent carbonate factories (Reijmer and Everaars, 1991; Reijmer, 1998; Preto, 2012). Fragments of carbonate with clotted peloidal fabric, oncoids, calcimicrobes such as *Girvanella*, *Cayeuxia* and *Tubiphytes* were considered microbially-derived carbonates, according to the criteria of Preto (2012). Of the remainder of the carbonate grains, ooids and mollusk fragments are the most common. According to Duguid et al. (2010), ooids are considered abiotic grains.

The composition of the grainstones and packstones displays sharp changes in the Milieres section. Facies that are dominated by microbial carbonates at its base are replaced by oolites and skeletal grainstones with less than 10% of microbial-derived grains at its top (Fig. 4 and Supplementary Material, Table 3S). Five horizons of microbialitic mounds and biostromes, with thicknesses from a few centimeters to nearly one meter, are also documented, and all occur before the transition to oolitic-skeletal grainstones and packstones (Fig. 4). These petrographic data testify to a transition from dominantly microbial carbonate production to ooid-skeletal carbonate factories previously reported in the Dolomites area by Preto and Hinnov (2003) and Gattolin et al. (2013).

5. Discussion

5.1. Negative carbon isotope excursion at the onset of the CPE

The negative CIE in the bulk organic matter (OM) at Lunz (Austria) and Baltonfüred (Hungary) occurs in correspondence to the Julian 1–Julian 2 boundary (Fig. 3). The negative CIE interrupts a ~3‰ positive Ladinan–early Carnian $\delta^{13}C$ trend that matches the well-known similar positive long-term shift recorded by brachiopod calcite, which has been linked to increased carbon burial after the Early Triassic "coal gap" (Korte et al., 2005; Preto et al., 2009; Dal Corso et al., 2011, 2012). The $\delta^{13}C_{TOC}$ curves from Austria and Hungary can be readily correlated to the existing bulk organic matter and biomarker $\delta^{13}C$ curves retrieved in the Dolomites (Figs. 5 and 6). The biostratigraphic correlation of the successions (see Supplementary Data for a detailed explanation) strongly suggests that the negative CIE occurred synchronously in the studied basins, at the boundary between the Julian 1 and the Julian 2 substages (Fig. 5).

In the studied sections, the CIE displays different magnitudes (Fig. 5). At Lunz and Baltonfüred it is 4.1‰ and 1.8‰ respectively (Fig. 5). In the Dolomites the $\delta^{13}C$ shift has a magnitude of ~4‰ in higher plant and marine lipids and 1.5‰ in the bulk organic matter (Dal Corso et al., 2012 and Fig. 6), although the initial part of the negative CIE could be missing (Fig. 5). These differences may be related to changes in the biological source of the OM deposited into the basins (e.g. Kürschner et al., 2007; Smith et al., 2007; van de Schootbrugge et al., 2008; French et al., 2014). For example, negative $\delta^{13}C_{TOC}$ shifts associated with the end-Triassic mass extinction show different amplitudes in

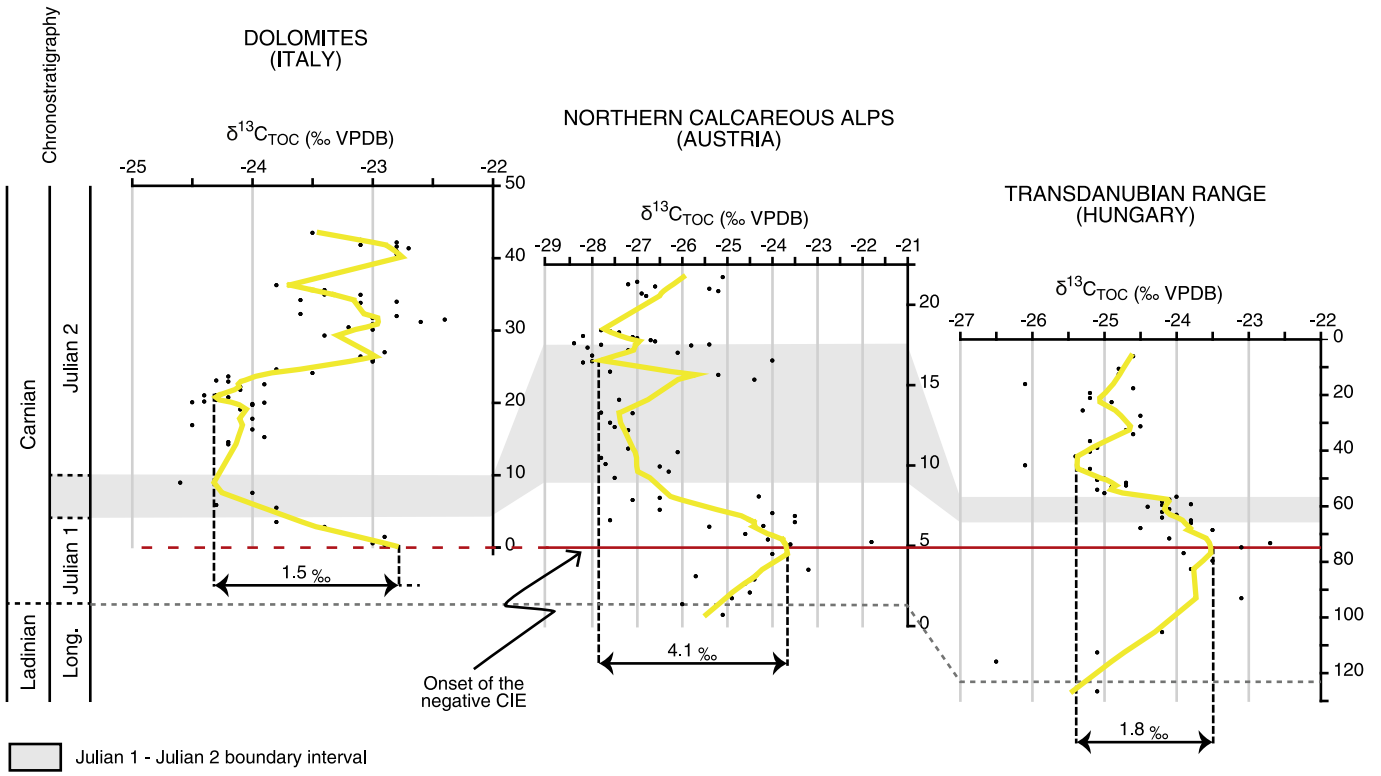

Fig. 5. Correlation of the $\delta^{13}C_{TOC}$ curves from Austria and Hungary (this study) with the $\delta^{13}C_{TOC}$ curve from the Dolomites in Italy (Dal Corso et al., 2012). *X*-axis does not have the same scale in order to compare the fine features of the curves. Note the differences in magnitude of the negative CIEs in the studied locations. The precise onset of the CIE is well defined in Austria and Hungary but not in the Dolomites where the base of the Milieres section does not crop out well (Dal Corso et al., 2012). A weighted least squares function (±15%) was applied to fit a curve to the data. Vertical scale in meters.

different depositional settings (Ruhl et al., 2009). This has been interpreted as evidence of changing proportions of marine and terrestrial OM in proximal and distal settings, since terrestrial and marine OM has different $\delta^{13}C$ signatures depending on the source of the inorganic carbon that is fixed, and on the isotopic fractionation occurring during photosynthesis. Today, terrestrial OM synthesized from atmospheric CO_2 ($\delta^{13}C = -7‰$) is more ^{13}C-depleted then marine OM synthesized from dissolved inorganic carbon ($\delta^{13}C = 0‰$) (e.g. Meyers, 1994), but evidence exists that before the Cretaceous terrestrial OM could have been more ^{13}C-enriched then marine OM (Arthur et al., 1985). The increase in the proportion of the terrigenous sediment fraction that occurs in all of the studied locations corresponds to the onset of the CPE (Fig. 2) and could therefore have changed the relative abundance of terrestrial and marine OM in the different basins, depending on the catchment area and the proximity of the section to the palaeo-shoreline. The magnitude of negative CIEs can also be modulated by changes in the terrestrial and marine community structure: e.g. the end-Triassic negative CIE recorded by bulk organic matter from Mingolsheim core in Germany is strongly correlated to the relative abundance of different palynomorph taxa (Van de Schootbrugge et al., 2008). Moreover, higher plants can amplify negative CIEs by up to ~2‰ due to increasing ^{13}C-discrimination under high humidity conditions (Bowen et al., 2004). However, the magnitude of the negative CIE recorded in terrestrial and marine biomarkers is similar (Dal Corso et al., 2012). This suggests that changes in land plant community composition, water stress, or photosynthetic isotopic fractionation did not modulate the higher plant signal at Milieres (e.g. Smith et al., 2007; Jenkyns, 2010).

Diagenetic processes are unlikely to have produced large changes in the $\delta^{13}C$ signature of the bulk OM in the studied sections. Laboratory studies have demonstrated that the $\delta^{13}C$ of OM is insensitive to thermal maturation, showing either no changes of the pristine $\delta^{13}C$ value, or small amounts of ^{13}C-enrichment (Lewan, 1983; Galimov, 2006). Major changes occur at late diagenetic and metamorphic stages. For example, shales and coals at the contact with magmatic intrusions show a 1–2‰ ^{13}C-enrichment because the thermal stress destroys $^{12}C-^{12}C$ bonds more rapidly than others C–C bonds (McKirdy and Powell, 1974; Simoneit et al., 1978; Saxby and Stephenson, 1987). Hence, thermal alteration of the OM cannot account for the synchronous negative CIE and the almost perfect biostratigraphically-constrained parallelism between the $\delta^{13}C_{TOC}$ curves presented in this work (Fig. 6).

In summary, local changes in the composition of OM could have modulated the magnitude of the negative CIE in the different geological settings, but the robust inter-regional biostratigraphic correlation of the sections substantiates the presence of a global organic-CIE in line with the conclusions of Dal Corso et al. (2012). Such a global event is expected to be recorded in other coeval sedimentary successions worldwide and to occur synchronously. The new isotopic data also allow a more precise examination of the temporal relationships between the carbon cycle perturbation and the sedimentological changes at the onset of the CPE (see later sections).

The presence of the CIE in both marine and terrestrial biomarkers suggests a CIE driven by the release of isotopically light CO_2 into the atmosphere (Dal Corso et al., 2012). This should also produce a similar response in the carbon isotopic composition of marine carbonates, but such an excursion is yet to be convincingly demonstrated during the CPE. The $\delta^{13}C_{CARB}$ curve from Milieres section does not parallel the $\delta^{13}C_{TOC}$ curve, not showing the negative CIE (Fig. 4). Similarly, previously published Carnian $\delta^{13}C_{CARB}$ from Austria, Southern Italy and India do not record any significant changes across the onset of the CPE (Hornung and Brandner, 2005; Keim et al., 2006; Hornung et al., 2007a; Preto et al., 2009). An exception is the negative ~2‰ $\delta^{13}C_{CARB}$ recorded in the continuous carbonate succession at Aghia Marina in Greece that could be compatible with the negative CIE recorded in organic materials (Muttoni et al., 2014). However, the stratigraphic correlation of the Greek carbonate $\delta^{13}C$ curve with the organic $\delta^{13}C$ curves of the northwestern Tethys is uncertain because the biostratigraphic constrains do

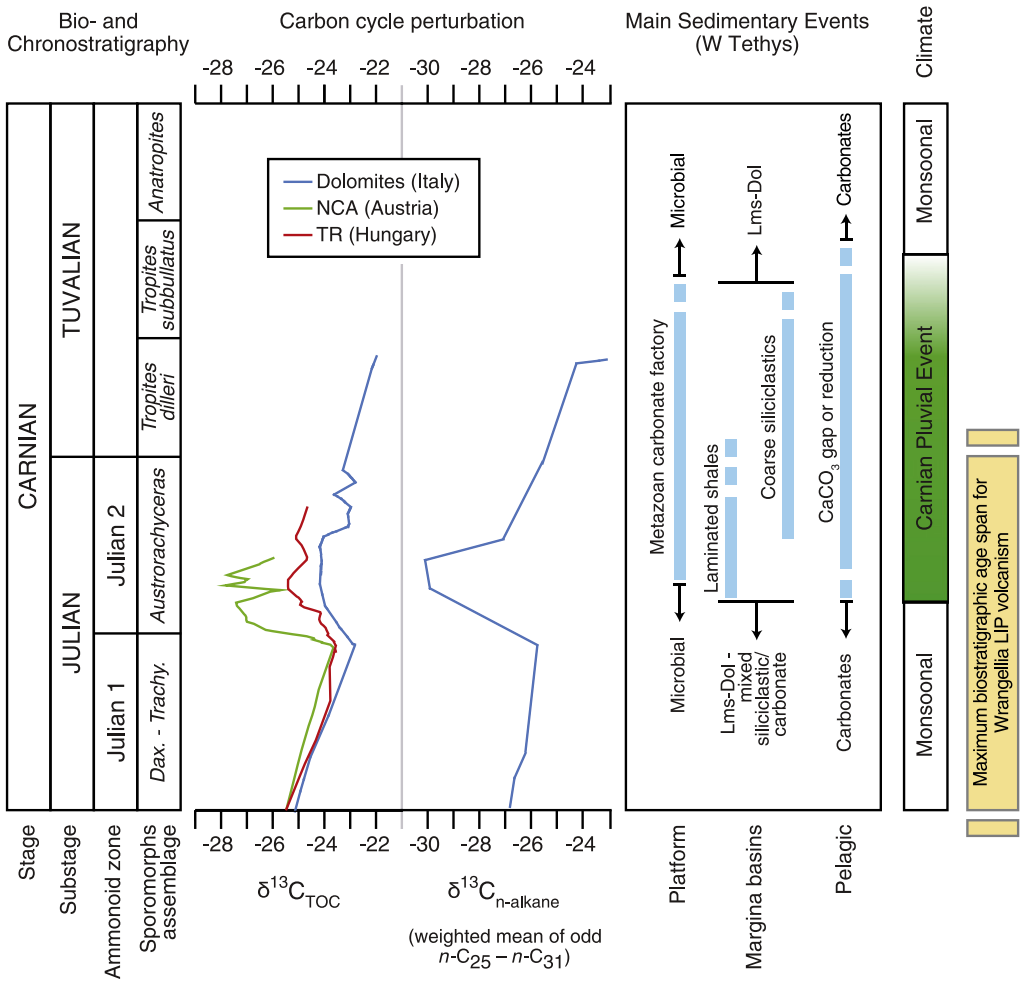

Fig. 6. $\delta^{13}C_{TOC}$ and higher plant *n*-alkanes curves from the northwestern Tethys and the major sedimentological changes that mark the CPE on land and ocean. The negative CIE marks the onset of the CPE. The maximum age span for Wrangellia volcanism is biostratigraphically constrained to the uppermost Ladinian–early Carnian (Julian) by the presence of *Daonella* (bivalve) in the silicified shales below the first basalts and of ammonoids of the *Tropites dilleri* zone in the intravolcanic and overlying limestone beds (e.g. Carlisle and Susuki, 1974; Tozer, 1994; Greene et al., 2010). NCA = Northern Calcareous Alps; TR = Transdanubian Range. Lms = limestone. Dol = dolomite.

not allow correlation of the sections at a resolution higher than substage level (Fig. 4S in Supplementary Data). In addition, a strong correlation between $\delta^{13}C_{CARB}$ and $\delta^{18}O_{CARB}$ exists in the interval of the negative CIE at Aghia Marina, pointing to a possible diagenetic alteration of the primary signal (Marshall, 1992). Moreover, these carbon isotope data don't record the positive ~3‰ Ladinian–early Carnian long-term shift that is a reproducible feature of the Triassic $\delta^{13}C$ curve (Korte et al., 2005; Preto et al., 2009; Dal Corso et al., 2011, 2012; Fig. 4S in Supplementary Data).

Reliable $\delta^{13}C_{CARB}$ curves are difficult to retrieve across the CPE because of a lack of sufficiently continuous carbonate successions. Bulk carbonates may also not accurately reflect the original global seawater $\delta^{13}C$ (e.g. Swart and Eberli, 2005; Swart 2008), either because in the Triassic "Neritan Ocean" carbonate production was restricted to shallow water biogenic precipitation (Zeebe and Westbroek, 2003), or because of isotopic changes that occur during early diagenesis of carbonates (e.g. Preto et al., 2009).

It is possible that a negative excursion in marine carbonate is absent rather than obscured by a lack of suitable material or diagenesis. Following the model proposed by Kump and Arthur (1999), a negative $\delta^{13}C_{TOC}$ not accompanied by a similar negative shift in marine carbonates could be interpreted as evidence of increasing pCO_2 levels. The absence of a carbonate carbon isotope excursion could be therefore be consistent with an introduction of volcanic CO_2 into the system as suggested by Dal Corso et al. (2012). However, other biogeochemical models for the end of the Triassic failed to obtain a similar discrepancy between the $\delta^{13}C$ responses of OM and carbonates to volcanic activity (Beerling and Berner, 2002).

Thus, the current lack of a convincing negative carbonate-carbon isotope excursion may be due to one of several factors: its absence; a lack of resolution in current records; a rarity of suitable material of exactly the right age; or diagenetic re-setting. This situation bears a distinct similarity to the evolution of the debate on the origin of the early Toarcian (Early Jurassic) marine organic carbon isotope excursion, where a pronounced negative organic-CIE was well documented before convincing evidence of an excursion in carbonate was found (see Newton and Bottrell, 2007 for a summary of the historic debate and Ullmann et al., 2014 and references therein for later work and a possible resolution).

The presence of the negative CIE in both the marine and the terrestrial biomarker data of Dal Corso et al (2012) strongly suggests that the discovery of a negative carbonate excursion awaits the analysis of an appropriate section: Their record is difficult to explain by anything other than a global perturbation of the carbon cycle and the release of CO_2 enriched in ^{12}C. The wider presence of the organic-CIE confirmed in the current study reinforces this conclusion.

5.2. ^{13}C-depleted CO_2 from Wrangellia LIP volcanism?

As proposed by Dal Corso et al. (2012), the most likely source of ^{13}C-depleted carbon in the Carnian is the roughly coeval volcanic activity of the Wrangellia oceanic plateau. Wrangellia flood basalts today outcrops in northwestern America, in a belt encompassing British Columbia, Yukon and Alaska (see geological maps in Greene et al., 2010). It is thought to have outpoured ~$1x10^6$ Km^3 of basalt in an interval of ~2 Ma, but the original volume of erupted basalts could be largely underestimated because part of the volcanic products could have been subducted during the Late Jurassic–Early Cretaceous Wrangellia accretion to the western North America (Lassiter et al., 1995; Greene et al., 2010). The sedimentary rocks that underlie and overlie Wrangellia flood basalts contain diagnostic fossils that constrain the age of LIP volcanism (Fig. 6). Below the basalts, silicified shale bear bivalves of the genus *Daonella*, which is diagnostic of the Ladinian. Within and above the last basalt flows, the limestone belonging to the Quatsino Fm. contains rich ammonoid fauna of the *Tropites dilleri* zone (including *T. dilleri*) indicating a lowermost Tuvalian age (Fig. 6; Carlisle and Susuki, 1974; Tozer, 1994). The age of Wrangellia volcanism can be thus biostratigraphycally constrained to the late Ladinian–early Tuvalian. $^{187}Os/^{188}Os$ data also suggests that the LIP volcanism is likely to have started in the late Ladinian (Xu et al., 2014). However, the $^{187}Os/^{188}Os$ shift that the authors interpret as the evidence of the onset of Wrangellia activity relies on one data point that is dated to the Ladinian by the presence of one north-American ammonoid (*Nathorstites* sp. Juv.), and thus needs further verification in other settings. The few radioisotopic ages ($^{40}Ar/^{39}Ar$ and U-Pb) of Wrangellia basalts and intrusive rocks that are likely to have retained a magmatic age are between 233 and 227 Ma (Greene et al., 2010 and references therein). However, due to the uncertainties that still exist on the Late Triassic chronology (Gradstein et al., 2012; Ogg et al., 2014), these radiometric ages cannot be univocally pinned to the Late Triassic biostratigraphy. Therefore, only a maximum biostratigraphic age span for Wrangellia volcanism is represented in Fig. 6.

If the estimates of Wrangellia LIP onset based on biostratigraphic constrains and $^{187}Os/^{188}Os$ data are realistic, it means that around 5–7 Myr elapsed between the onset of volcanism and the start of the CPE (Fig. 6) according to the current Geologic Time Scale (Gradstein et al., 2012). This raises many questions about the mechanisms that triggered the carbon cycle disruption and climate change in the Carnian. A long lasting late Ladinian–late Carnian Wrangellia volcanism may have slowly increased pCO_2 to the critical temperature when methane hydrates in the ocean floor could have been released. Alternatively, the CIE might have been the expression of a temporary peak in volcanic activity, or of a change in the style of the volcanism. Notably, the Wrangellia volcanic products show a general evolution from submarine to subaerial–shallow water (Greene et al., 2010). The understanding of these mechanisms is beyond the scope of this paper, and more geochronological and modeling studies are required to define the precise temporal and cause-and-effect relationships between the eruptive phases of Wrangellia LIP and the CPE. Nevertheless, existing age constraints show that Carnian LIP volcanism and climate change overlapped (Fig. 6), strongly suggesting a causal link between the two. The question whether LIP CO_2 alone and/or the release of CH_4 from dissociation of ocean floor clathrates could have caused the negative CIE, previously discussed in Dal Corso et al. (2012), cannot be addressed until the carbon isotope composition of Wrangellia CO_2 and the amount of ocean floor clathrates in the Carnian can be estimated.

5.3. Carbon cycle perturbation and increased rainfall

Our results are consistent with a causal link between a carbon isotope perturbation in the Earth surface reservoirs of exchangeable carbon, maybe from LIP volcanism, and the onset of the CPE. These results imply a classic scenario of climate response to pCO_2 rise, similar to that suggested for others events of the Phanerozoic (e.g., Jenkyns, 2010).

Indeed, the transfer of CO_2 into the reservoirs of the active carbon cycle could have triggered the warming recorded by the $\delta^{18}O$ of conodont apatite (Hornung et al., 2007b; Rigo and Joachimski, 2010), and a subsequent increase in the total column water vapor in the atmosphere, which exerts a positive feedback on the greenhouse effect and provides more precipitable water in the atmosphere (Trenberth, 2011). Today, rainfall datasets and climate modeling suggest that, due to this mechanism, the frequency and magnitude of heavy rains and consequent floods increase with rising CO_2 and global warming, with this effect being particularly strong in monsoonal areas (e.g. Goswami et al., 2006; Trenberth, 2011; Lau et al., 2013). By analogy, the results of this study suggest that in the Carnian the introduction of CO_2 into the atmosphere–ocean system is likely to have increased rainfall by intensification of Pangaea mega-monsoon activity, thus enhancing continental weathering and river discharge.

5.4. Oxygen-depletion and massive siliciclastic sedimentation in marginal basins

At Lunz, the onset of the CIE occurs at the top of the nodular limestones of the Reifling Fm., below the laminated marly limestones of the Göstling Fm. (Fig. 3). Similarly, in Bfü-1 borehole, the CIE starts in the uppermost part of the Füred Limestone, just below the laminated marly limestones at the base of the Veszprém Fm. (Fig. 3). This evidence highlights that the change from carbonate to siliciclastic sedimentation (Fig. 3) is coincident to the global carbon cycle perturbation and occurred almost synchronously in the studied basins.

The deposition of laminated black shale (TOC up to 4.7% according to Hornung and Brandner, 2005) in Austria shortly after the initiation of the negative organic-CIE indicates oxygen-depletion that may have been driven by an increased flux of nutrients into the basin as a consequence of enhanced continental weathering (Hornung et al., 2007b). A similar pattern can be observed also in the Transdanubian Range (Hungary), although true oxygen depletion seems to have developed only in the restricted Zsámbék Basin (Rostási et al., 2011). Probable low-oxygen conditions have also been documented in other restricted basins of Tethys: in the Dolomites, where dark claystones with abundant pyrite were deposited when the climatic conditions became more humid (Bizzarini and Laghi, 2005; Keim et al., 2006; Neri et al., 2007); in Tunisia, where organic-rich black shales are found within early Carnian successions (Soua, 2014); in the lower Rama Fm. of the Spiti basin in India, where laminated shales have been biostratigraphically correlated with the Austrian Reingraben shales (Hornung et al., 2007a); and also in the South China Block (Great Bank of Guizhou), where black shales were deposited in the Carnian (Wang et al., 2008). In contrast to the situation in marginal basins, there is no evidence of anoxia during the CPE in the open ocean (Rigo et al., 2007; Nakada et al., 2014). This suggests that oxygen depletion developed only in marginal settings of the Tethys, while the open ocean remained unaffected. Indeed, paleogeography might have played an important role in the variable development of anoxia by favoring the water-mass stratification and oxygen-depletion in basins with restricted circulation, as the case of many Jurassic–Cretaceous OAEs nicely shows (Jenkyns, 2010).

In the Northern Calcareous Alps the phase of oxygen depletion (documented by the Reingraben Fm.) was interrupted by the deposition of a thick series (up to 300 m) of coarse deltaic siliciclastic material (Lunz Fm., Fig. 2), whereas in the Transdanubian Range the deposition of marlstones and claystones of the Veszprém Fm. continued with up to 450 m of compacted fine siliciclastics (Fig. 2) with the only interruption being the 10–12 m thick Nosztor Limestone (Fig. 2). It's remarkable that this huge amount of terrigenous material was deposited in the relatively short time represented by the Julian 2 substage. In this time interval the basins were completely filled up, and the submarine

topography of the western Tethys was flattened, creating the conditions for in the development of a carbonate shelf and terrestrial sedimentation (Gianolla and Jacquin, 1998; Breda and Preto, 2011) (Fig. 2).

5.5. The crisis of microbial carbonate platforms

In Austria and Hungary, the arrival of siliciclastics and the oxygen depletion into the basins are coupled to a significant decrease of carbonate input (Schlager and Schöllnberger, 1974; Simms and Ruffell, 1989; Hornung et al., 2007a; Fig. 2). This could be interpreted as a dilution effect, however, decreasing carbonate input to the deep-water and the consequent rise of the CCD Lagonegro Basin have been linked to a crisis experienced by Tethysian carbonate systems during the CPE (Rigo et al., 2007; Fig. 6). This study shows that the start of this crisis corresponds directly with the initiation of the negative organic-CIE. Modal analysis of carbonates from Milieres section show that the relative abundance of microbial carbonates drops nearly to 0%, to be substituted by inorganic (ooids) and skeletal grains (Fig. 4). Contemporaneously, microbial mounds disappear in the Dolomites (Milieres section). In the western Tethys, early Carnian high-relief carbonate platforms disappeared at the CPE (e.g., Preto and Hinnov, 2003; Keim et al., 2006; Stefani et al., 2010). The early Carnian high-relief platforms of the Dolomites were essentially built by microbial carbonate factories (Russo et al., 1997; Keim and Schlager, 2001), hence the disappearance of microbial carbonate grains in the allochtonous carbonates of Milieres records this demise. At Milieres, the crisis of the microbial factories was synchronous with the negative CIE and the onset of climate change. Since significant pelagic calcification was still absent in the Carnian (Bown et al., 2004; Gardin et al., 2012; Preto et al., 2013), the production crisis of shallow-water carbonate systems would have led to a net decrease of the flux of carbonate to the deep ocean, that may explain the coeval rise of the CCD observed in deep water settings of the Lagonegro Basin (Rigo et al., 2007). It is not yet possible to unequivocally define the cause of such a widespread crisis of microbial carbonate factories. Neither the excess of nutrient supply, previously invoked to explain the Carnian carbonate platforms crisis (Keim and Schlager, 2001; Hornung et al., 2007a), nor oxygen depletion can explain the switch from microbial to metazoan factories. Higher nutrient concentrations and lower oxygenation may put coral reef ecosystems into crisis (Hallock and Schlager, 1986; Mutti and Hallock, 2003), but should not affect the microbial carbonate factories that thrived in nutrients-rich and poorly oxygenated waters throughout the Phanerozoic (Schlager, 2003). A recent study (Riding et al., 2014) highlighted that the decline of calcified bacterial crusts in Holocene tropical reefs seem to be closely linked to ocean acidification. A link between a decrease of seawater saturation state with respect to carbonate and the demise of microbial platforms at the CPE, in correspondence to the negative CIE, is an intriguing hypothesis that deserves future investigations.

6. Conclusions

This study shows that injection of ^{13}C-depleted CO_2 into the atmosphere-ocean system is synchronous with the onset of the Carnian Pluvial Event in three western Tethys basins and provides further evidence of the global nature of this isotopic event. The initiation of the organic-carbon isotope excursion prior to increased clastic sedimentation, oxygen depletion and changes in carbonate production is consistent with a rapid carbon cycle disruption triggering a change to a much wetter climate. This would have in turn resulted in increased continental weathering, and increases in sediment and nutrient fluxes into the ocean that are likely to have brought about the rapid infilling of the basins and produced oxygen depleted conditions in some marginal basin settings. This period of climate change, now widely documented within the Late Triassic paleotropics, may be viewed as an intensification of Pangean mega-monsoonal activity, and triggered a poorly understood crisis of microbial carbonate platforms.

Acknowledgments

This work was funded by a "Young Researcher Grant" (DALCPRGR12) of the University of Padova (P.I.: JDC). Fieldwork of PG and MC was funded by PRIN (20107ESMX9_003). Petrographic work by NP was funded by the Alexander von Humboldt Foundation. Thanks go to C. Betto (UNIPD) and A. Fiore (UNIFE) for assistance in samples preparation. We gratefully acknowledge the reviews of J.G. Ogg and an anonymous reviewer, which greatly helped to improve the paper.

Appendix A. Supplementary data

Supplementary data to this article can be found online at http://dx.doi.org/10.1016/j.gloplacha.2015.01.013.

References

Arche, A., López-Gómez, J.L., 2014. The Carnian Pluvial Event in Western Europe: new data from Iberia and correlation with the Western Neotethys and Eastern North America–NW Africa regions. Earth-Sci. Rev. 128, 196–231. http://dx.doi.org/10.1016/j.earscirev.2013.10.012.

Arthur, M.A., Dean, W.E., Claypool, G.E., 1985. Anomalous ^{13}C enrichment in modern marine organic carbon. Nature 315, 216–218. http://dx.doi.org/10.1038/315216a0.

Beerling, D.J., Berner, R.A., 2002. Biogeochemical constraints on the Triassic–Jurassic boundary carbon cycle event. Glob. Biogeochem. Cycles 16 (3), 1036. http://dx.doi.org/10.1029/2001GB001637.

Bialik, O., Korngreen, D., Benjamini, C., 2013. Carnian (Triassic) aridization on the Levant margin; evidence from the M1 member, Mohilla Formation, Makhtesh Ramon, south Israel. Facies 59, 559–581. http://dx.doi.org/10.1007/s10347-012-0321-5.

Bizzarini, F., Laghi, G.F., 2005. La successione "Cassiana" nell'area a nord di Misurina (Trias, Dolomiti). Lav. Soc. Venez. Sci. Nat. 30, 127–143.

Bowen, G.J., Beerling, D.J., Koch, P.L., Zachos, J.C., Quattlebaum, T., 2004. A humid climate state during the Palaeocene/Eocene thermal maximum. Nature 432, 495–499. http://dx.doi.org/10.1038/nature03115.

Bown, P.R., Lees, J.A., Young, J.R., 2004. Calcareous nannoplankton evolution and diversity through time. In: Thierstein, H.R., Young, J.R. (Eds.), Coccolithophores — From Molecular Processes To Global Impact. Springer Verlag, Berlin, pp. 481–505.

Breda, A., Preto, N., 2011. Anatomy of an Upper Triassic continental to marginal-marine system: the mixed siliciclastic–carbonate Travenanzes Formation (Dolomites, Northern Italy). Sedimentology 58, 1613–1647. http://dx.doi.org/10.1111/j.1365-3091.2011.01227.x.

Breda, A., Preto, N., Roghi, G., Furin, S., Meneguolo, R., Ragazzi, E., Fedele, P., Gianolla, P., 2009. The Carnian Pluvial Event in the Tofane area (Cortina d'Ampezzo, Dolomites, Italy). Geol. Alps 6, 80–115.

Budai, T., Császár, G., Csillag, G., Dudko, A., Koloszár, L., Majoros, G., 1999. Geology of the Balaton Highland. Occasional Papers. Geological Institute of Hungary, Budapest, p. 197.

Carlisle, D., Susuki, T., 1974. Emergent basalt and submergent carbonate-clastic sequences including Upper Triassic Dilleri and Welleri Zones on Vancouver Island. Can. J. Earth Sci. 11, 254–279.

Csontos, L., Vörös, A., 2004. Mesozoic plate tectonic reconstruction of the Carpathian region. Palaeogeogr. Palaeoclimatol. Palaeoecol. 210, 1–56. http://dx.doi.org/10.1016/j.palaeo.2004.02.033.

Dal Corso, J., Preto, N., Kustatscher, E., Mietto, P., Roghi, G., Jenkyns, H.C., 2011. Carbon-isotope variability of Triassic amber, as compared with wood and leaves (Southern Alps, Italy). Palaeogeogr. Palaeoclimatol. Palaeoecol. 302, 187–193. http://dx.doi.org/10.1016/j.palaeo.2011.01.007.

Dal Corso, J., Mietto, P., Newton, R.J., Pancost, R.D., Preto, N., Roghi, G., Wignall, P.B., 2012. Discovery of a major negative $\delta^{13}C$ spike in the Carnian (Late Triassic) linked to the eruption of Wrangellia flood basalts. Geology 40, 79–82. http://dx.doi.org/10.1130/G32473.1.

Duguid, S.M.A., Kyser, T.K., James, N.P., Rankey, E.C., 2010. Microbes and ooids. J. Sediment. Res. 80, 236–251. http://dx.doi.org/10.2110/jsr.2010.027.

Franz, M., Nowak, K., Berner, U., Haunisch, C., Bandel, K., Rohling, H.G., Wolfgramm, M., 2014. Eustatic control on epicontinental basins: the example of the Stuttgart Formation in the Central European Basin (Middle Keuper, Late Triassic). Glob. Planet. Chang. 122, 305–329. http://dx.doi.org/10.1016/j.gloplacha.2014.07.010.

French, K.L., Sepulveda, J., Trabucho-Alexandre, J., Grocke, D.R., Summons, R.E., 2014. Organic geochemistry of the early Toarcian oceanic anoxic event in Hawsker Bottoms, Yorkshire, England. EPSL 390, 116–127. http://dx.doi.org/10.1016/j.epsl.2013.12.033.

Furin, S., Preto, N., Rigo, M., Roghi, G., Giannola, P., Crowley, J.L., Bowring, S.A., 2006. High-precision U–Pb zircon age from the Triassic of Italy: implications for the Triassic time scale and the Carnian origin of calcareous nannoplankton and dinosaurs. Geology 34, 1009–1012. http://dx.doi.org/10.1130/G22967A.1.

Galimov, E.M., 2006. Isotope organic geochemistry. Org. Geochem. 37, 1200–1262. http://dx.doi.org/10.1016/j.orggeochem.2006.04.009.

Gardin, S., Krystyn, L., Richoz, S., Bartolini, A., Galbrun, B., 2012. Where and when the earliest coccolithophores? Lethaia 45, 507–523.

Gattolin, G., Breda, A., Preto, N., 2013. Demise of Late Triassic carbonate platforms triggered the onset of a tide-dominated depositional system in the dolomites, northern Italy. Sediment. Geol. 297, 38–49. http://dx.doi.org/10.1016/j.sedgeo.2013.09.005.

Gianolla, P., Jacquin, T., 1998. Triassic sequence stratigraphic framework of Western European basins. In: Graciansky, De, et al. (Eds.), Mesozoic And Cenozoic Sequence Stratigraphy Of European Basins. SEPM Special Publication 60, pp. 643–650.
Góczán, F., Oravecz-Scheffer, A., Csillag, G., 1991. The stratigraphic characterization of the Cordevolian and Julian Formations of Csukréti Ravine, Balatoncsicsó. Földt. Int. Évi Jel. 241–323 (-ról).
Goswami, B.N., Venugopal, V., Sengupta, D., Madhusoodanan, M.S., Xavier, P.K., 2006. Increasing trend of extreme rain events over India in a warming environment. Science 314, 1442–1445. http://dx.doi.org/10.1126/science.1132027.
Gradstein, F., Ogg, J., Schmitz, M., Ogg, G., 2012. The Geologic Time Scale. Elsevier, Amsterdam.
Greene, A.R., Scoates, J.S., Weis, D., Katvala, E.C., Israel, S., Nixon, G.T., 2010. The architecture of oceanic plateaus revealed by the volcanic stratigraphy of the accreted Wrangellia oceanic plateau. Geosphere 6, 47–73. http://dx.doi.org/10.1130/GES00212.1.
Haas, J., Budai, T., Raucsik, B., 2012. Climatic controls on sedimentary environments in the Triassic of the Trasdanubian Range (Western Hungary). Palaeogeogr. Palaeoclimatol. Palaeoecol. 353–355, 31–44. http://dx.doi.org/10.1016/j.palaeo.2012.06.031.
Hallock, P., Schlager, W., 1986. Nutrient excess and the demise of coral reefs and carbonate platforms. Palaios 1, 389–398. http://dx.doi.org/10.2307/3514476.
Hornung, T., Brandner, R., 2005. Biochronostratigraphy of the Reingraben Turnover (Hallstatt Facies Belt): local black shale events controlled by regional tectonics, climatic change and plate tectonics. Facies 51, 460–479. http://dx.doi.org/10.1007/s10347-005-0061-x.
Hornung, T., Krystyn, L., Brandner, R., 2007a. A Tethys-wide mid-Carnian (Upper Triassic) carbonate productivity decline: evidence for the Alpine Reingraben Event from Spiti (Indian Himalaya). J. Asian Earth Sci. 30, 285–302. http://dx.doi.org/10.1016/j.jseaes.2006.10.001.
Hornung, T., Brandner, R., Krystyn, L., Joachimsky, M.M., Keim, L., 2007b. Multistratigraphic constraints on the NW Tethyan "Carnian Crisis". N. M. Mus. Nat. Hist. Sci. Bull. 4, 9–67.
Jenkyns, H.C., 2010. Geochemistry of oceanic anoxic events. Geochem. Geophys. Geosyst. 11 (3), Q03004. http://dx.doi.org/10.1029/2009GC002788.
Keim, L., Schlager, W., 2001. Quantitative compositional analysis of a Triassic carbonate platform (Southern Alps, Italy). Sediment. Geol. 139, 261–283. http://dx.doi.org/10.1016/S0037-0738(00)00163-9.
Keim, L., Spötl, C., Brandner, R., 2006. The aftermath of the Carnian carbonate platform demise: a basinal perspective (Dolomites, Southern Alps). Sedimentology 53, 361–386. http://dx.doi.org/10.1111/j.1365-3091.2006.00768.x.
Köppen, A., 1997. Faziesentwicklung in der frühen Obertrias Mitteleuropas-ein sequenzstratigraphischer Vergleich. Gaea Heidelbergensis 2, 1–233.
Korte, C., Kozur, H.W., Veizer, J., 2005. $\delta^{13}C$ and $\delta^{18}O$ values of Triassic brachiopods and carbonate rocks as proxies for coeval seawater and palaeotemperature. Palaeogeogr. Palaeoclimatol. Palaeoecol. 226, 287–306.
Krystyn, L., 1991. Die Fossillagerstätten der alpinen Trias: Exkursionsführer. Universität Wien, p. 61.
Krystyn, L., 1978. Eine neue Zonengliederung im alpin-mediterranen Unterkan. In: Zapfe, E. (Ed.), Beiträge zur Biostratigraphie der Tethys-Trias. Springer, Wien.
Kump, L.R., Arthur, M.A., 1999. Interpreting carbon-isotope excursions: carbonates and organic matter. Chem. Geol. 161, 181–198.
Kürschner, W., Bonis, N., Krysytn, L., 2007. Carbon isotope stratigraphy and palynostratigraphy of the Triassic–Jurassic transition in the Tiefengraben section—Northern Calcareous Alps (Austria). Palaeogeogr. Palaeoclimatol. Palaeoecol. 244, 257–280. http://dx.doi.org/10.1016/j.palaeo.2006.06.031.
Kutzbach, J.E., Gallimore, R.G., 1989. Pangean climates: megamonsoons of the megacontinent. J. Geophys. Res. Atmos. 94, 3341–3357. http://dx.doi.org/10.1029/JD094iD03p03341.
Lassiter, J.C., DePaolo, D.J., Mahoney, J.J., 1995. Geochemistry of the Wrangellia flood basalt province: implications for the role of continental and oceanic lithosphere in flood basalt genesis. J. Petrol. 36, 983–1009. http://dx.doi.org/10.1093/petrology/36.4.983.
Lau, W.K.-M., Wu, H.-T., Kim, K.-M., 2013. A canonical response of precipitation characteristics to global warming from CMIP5 models. Geophys. Res. Lett. 40, 3163–3169. http://dx.doi.org/10.1002/grl.50420.
Lewan, M.D., 1983. Effects of thermal maturation on stable organic carbon isotopes as determined by hydrous pyrolysis of Woodford Shale. Geochim. Cosmochim. Acta 47, 1471–1479.
Lukeneder, S., Lukeneder, A., 2013. A new ammonoid fauna from the Carnian (Upper Triassic) Kasimlar Formation of the Taurus Mountains (Anatolia, Turkey). Palaeontology 57, 357–396. http://dx.doi.org/10.1111/pala.12070.
Lukeneder, S., Lukeneder, A., Harzhauser, M., Islamoglu, Y., Krystyn, L., Lein, R., 2012. A delayed carbonate factory breakdown during the Tethyan-wide Carnian Pluvial Episode along the Cimmerian terranes (Taurus, Turkey). Facies 58, 279–296. http://dx.doi.org/10.1007/s10347-011-0279-8.
Marshall, J.D., 1992. Climatic and oceanographic isotopic signals from the carbonate rock record and their preservation. Geol. Mag. 129, 151–162. http://dx.doi.org/10.1017/S0016756800008244.
McKirdy, D.M., Powell, T.G., 1974. Metamorphic alteration of carbon iso-topic composition in ancient sedimentary organic matter: new evidence from Australia and South Africa. Geology 2, 591–595.
Meyers, P.A., 1994. Preservation of elemental and isotopic source identification of sedimentary organic matter. Chem. Geol. 114, 289–302.
Mutti, M., Hallock, P., 2003. Carbonate systems along nutrient and temperature gradients: some sedimentological and geochemical constraints. Int. J. Earth Sci. 92, 465–475. http://dx.doi.org/10.1007/s00531-003-0350-y.
Muttoni, G., Mazza, M., Mosher, D., Katz, M.E., Kent, D.V., Balini, M., 2014. A Middle–Late Triassic (Ladinian–Rhaetian) Carbon and Oxygen isotope record from the Tethyan Ocean. Palaeogeogr. Palaeoclimatol. Palaeoecol. 399, 246–259. http://dx.doi.org/10.1016/j.palaeo.2014.01.018.
Nakada, R., Ogawa, K., Suzuki, N., Takahashi, S., Takahaschi, Y., 2014. Late Triassic compositional changes of aeolian dusts in the pelagic Panthalassa: response to the continental climatic change. Palaeogeogr. Palaeoclimatol. Palaeoecol. 393, 61–75. http://dx.doi.org/10.1016/j.palaeo.2013.10.014.
Neri, C., P. Gianolla, S. Furlanis, R. Caputo and A. Bosellini, 2007. Note Illustrative della Carta Geologica d'Italia alla scala 1:50.000, Foglio 029 Cortina d'Ampezzo. SystemCart, 200 p., Roma, A.P.A.T.
Newton, R.J., Bottrell, S., 2007. Stable isotopes of carbon and sulphur as indicators of environmental change: past and present. J. Geol. Soc. 164, 691–708. http://dx.doi.org/10.1144/0016-76492006-101.
Ogg, J.G., Huang, C., Hinnov, L., 2014. Triassic timescale status: a brief overview. Albertiana 41, 3–30.
Pott, C., Krings, M., Kerp, H., 2008. The Carnian (Late Triassic) flora from Lunz in Lower Austria: paleoecological considerations. Palaeoworld 17, 172–182. http://dx.doi.org/10.1016/j.palwor.2008.03.001.
Preto, N., 2012. Petrology of carbonate beds from the stratotype of the Carnian (Stuores Wiesen section, Dolomites, Italy): the contribution of platform-derived microbialites. Geol. Alps 9, 12–29.
Preto, N., Hinnov, L., 2003. Unrevealing the origin of carbonate platform cyclothemes in the Upper Triassic Durrenstein Formation (Dolomites, Italy). J. Sediment. Res. 73, 774–789. http://dx.doi.org/10.1306/030503730774.
Preto, N., Spötl, C., Guaiumi, C., 2009. Evaluation of bulk carbonate $\delta^{13}C$ data from Triassic hemipelagites and the initial composition of carbonate mud. Sedimentology 56, 1329–1345. http://dx.doi.org/10.1111/j.1365-3091.2008.01036.x.
Preto, N., Kustatscher, E., Wignall, P.B., 2010. Triassic climates—state of the art and perspectives. Palaeogeogr. Palaeoclimatol. Palaeoecol. 290, 1–10. http://dx.doi.org/10.1016/j.palaeo.2010.03.015.
Preto, N., Rigo, M., Agnini, C., Sprovieri, M., Westphal, H., 2013. The calcareous nannofossil *Prinsiosphaera* achieved rock-forming abundances in the latest Triassic of western Tethys: consequences for the $\delta^{13}C$ of bulk carbonate. Biogeosciences 10, 6053–6068.
Reijmer, J.J.G., 1998. Compositional variations during phases of progradation and retrogradation of a Triassic carbonate platform (Picco di Vallandro/Durrenstein, Dolomites, Italy). Geol. Rundsch. 87, 436–448. http://dx.doi.org/10.1007/PL00009941.
Reijmer, J.J.G., Everaars, J.S.L., 1991. Carbonate platform facies reflected in carbonate basin facies (Triassic, northern Calcareous Alps). Facies 25, 253–278. http://dx.doi.org/10.1007/BF02536761.
Riding, R., Liang, L., Braga, J.C., 2014. Millennial-scale ocean acidification and late Quaternary decline of cryptic bacterial crusts in tropical reefs. Geobiology http://dx.doi.org/10.1111/gbi.12097.
Rigo, M., Joachimski, M.M., 2010. Palaeoecology of Late Triassic conodonts: constraints from oxygen isotopes in biogenic apatite. Acta Palaeontol. Pol. 55, 471–478. http://dx.doi.org/10.4202/app.2009.0100.
Rigo, M., Preto, N., Roghi, G., Tateo, F., Mietto, P., 2007. A rise in the carbonate compensation depth of western Tethys in the Carnian: deep-water evidence for the Carnian Pluvial Event. Palaeogeogr. Palaeoclimatol. Palaeoecol. 246, 188–205. http://dx.doi.org/10.1016/j.palaeo.2006.09.013.
Roghi, G., 2004. Palynological investigations in the Carnian of Cave del Predil area (once Raibl, Julian Alps). Rev. Palaeobot. Palynol. 132, 1–35.
Roghi, G., Gianolla, P., Minarelli, L., Pilati, C., Preto, N., 2010. Palynological correlation of Carnian humid pulses throughout western Tethys. Palaeogeogr. Palaeoclimatol. Palaeoecol. 290, 89–106. http://dx.doi.org/10.1016/j.palaeo.2009.11.006.
Rostási, Á., Raucsik, B., Varga, A., 2011. Palaeoenvironmental controls on the clay mineralogy of Carnian sections from the Transdanubian Range (Hungary). Palaeogeogr. Palaeoclimatol. Palaeoecol. 300, 101–112. http://dx.doi.org/10.1016/j.palaeo.2010.12.013.
Rüffer, T., Bechstädt, T., 1998. Triassic sequence stratigraphy in the western part of the Northern Calcareous Alps (Austria). Mesozoic–Cenozoic Sequence Stratigraphy of European Basins 60 pp. 751–761.
Ruhl, M., Kürschner, W.M., Krystyn, L., 2009. Triassic–Jurassic organic carbon isotope stratigraphy of key sections in the western Tethys realm (Austria). EPSL 281, 169–187. http://dx.doi.org/10.1016/j.epsl.2009.02.020.
Russo, F., Neri, C., Mastandrea, A., Baracca, A., 1997. The mud mound nature of the Cassian platform margins of the Dolomites. A case history: the Cipit boulders from Punta Grohmann (Sasso Piatto Massif, Northern Italy). Facies 36, 25–36.
Saxby, J.D., Stephenson, L.C., 1987. Effect of an igneous intrusion on oil shale at Rundle (Australia). Chem. Geol. 63, 1–16.
Schlager, W., 2003. Sedimentology And Sequence Stratigraphy Of Reefs And Carbonate Platforms. Continuing Education Course Note Series #34. AAPG, Tulsa, Oklahoma, U.S.A.
Schlager, W., Schöllnberger, W., 1974. Das Prinzip stratigraphischer Wenden in der Schichtfolge der Nördlichen Kalkalpen. Mitt. Österr. Geol. Ges. 66–67, 165–193.
Sellwood, B.W., Valdes, P.J., 2006. Mesozoic climates: general circulation models and the rock record. Sediment. Geol. 190, 269–287. http://dx.doi.org/10.1016/j.sedgeo.2006.05.013.
Simms, M.J., Ruffell, A.H., 1989. Synchroneity of climatic change and extinctions in the Late Triassic. Geology 17, 265–268. http://dx.doi.org/10.1130/0091-7613.
Simms, M.J., Ruffel, A.H., Johnson, L.A., 1995. Biotic and climatic changes in the Carnian (Triassic) of Europe and adjacent areas. In: Fraser, N.C., Sues, H.-D. (Eds.), In The Shadow Of The Dinosaurs: Early Mesozoic Tetrapods. Cambridge University Press, pp. 352–365.
Simoneit, B.R.T., Brenner, S., Peters, K.E., Kaplan, I.R., 1978. Thermal alteration of Cretaceous black shale by basaltic intrusions in the Eastern Atlantic. Nature 273, 501–504. http://dx.doi.org/10.1038/273501a0.

Smith, F., Wing, S.L., Freeman, K.E., 2007. Magnitude of the carbon isotope excursion at the Paleocene–Eocene thermal maximum: the role of plant community change. EPSL 262, 50–60. http://dx.doi.org/10.1016/j.epsl.2007.07.021.

Soua, M., 2014. Early Carnian anoxic event as recorded in the southern Tethyan margin, Tunisia: an overview. Int. Geol. Rev. 56, 1884–1905. http://dx.doi.org/10.1080/00206814.2014.967315.

Stefani, M., Furin, S., Gianolla, P., 2010. The changing climate framework and depositional dynamics of the Triassic carbonate platforms from the Dolomites. Palaeogeogr. Palaeoclimatol. Palaeoecol. 290, 43–57. http://dx.doi.org/10.1016/j.palaeo.2010.02.018.

Swart, P.A., 2008. Global Synchronous changes in the carbon isotopic composition of carbonate sediments unrelated to changes in the global carbon cycle. PNAS 105 (37), 13741–13745. http://dx.doi.org/10.1073/pnas.0802841105.

Swart, P.K., Eberli, G., 2005. The nature of the $\delta^{13}C$ of periplatform sediments: implications for stratigraphy and the global carbon cycle. Sediment. Geol. 175, 115–129. http://dx.doi.org/10.1016/j.sedgeo.2004.12.029.

Tozer, E.T., 1994. Canadian Triassic Ammonoid Faunas: GSC Bulletin. p. 467.

Trenberth, K.A., 2011. Changes in precipitation with climate change. Clim. Res. 47, 123–138. http://dx.doi.org/10.3354/cr00953.

Ullmann, C.V., Nicolas, T., Ruhl, M., Hesselbo, S.P., Korte, C., 2014. Effect of a Jurassic oceanic anoxic event on belemnite ecology and evolution. PNAS 111 (28), 10073–10076. http://dx.doi.org/10.1073/pnas.1320156111.

van de Schootbrugge, B., Payne, J.L., Tomasovych, A., Pross, J., Fiebig, J., Benbrahim, M., Föllmi, K.B., Quan, T.M., 2008. Carbon cycle perturbation and stabilization in the wake of the Triassic–Jurassic boundary mass-extinction event. Geochem. Geophys. Geosyst. 9 (4), Q04028. http://dx.doi.org/10.1029/2007GC001914.

Van der Plas, L., Tobi, A.C., 1965. A chart for judging the reliability of point counting results. Am. J. Sci. 263, 87–90. http://dx.doi.org/10.2475/ajs.263.1.87.

Wang, X., Bachmann, G., Hagdorn, H., Sander, M., Cuny, G., Xiaohong, C., Chuanshang, W., Lide, C., Long, C., Fansong, M., Guanghong, X., 2008. The Late Triassic black shales of the Guanling area, Guizhou province, south-west China: a unique marine reptile and pelagic crinoid fossil lagerstätte. Palaeontology 51, 27–61. http://dx.doi.org/10.1111/j.1475-4983.2007.00735.x.

Xu, G., Hannah, J.L., Stein, H.J., Mørkd, A., Os Vigran, J., Bingen, B., Schutte, D., Lundschieng, B.A., 2014. Cause of Upper Triassic climate crisis revealed by Re–Os geochemistry of Boreal black shales. Palaeogeogr. Palaeoclimatol. Palaeoecol. 395, 222–232. http://dx.doi.org/10.1016/j.palaeo.2013.12.027.

Zeebe, R.E., Westbroek, P., 2003. A simple model for the $CaCO_3$ saturation state of the ocean: The "Strangelove", the "Neritan" and the "Cretan" Ocean. Geochem. Geophys. Geosyst. 4 (12), 1104. http://dx.doi.org/10.1029/2003GC000538.